Highlights

Accurate wavelet thresholding method for ECG signals

Kaimin Yu[a], Lei Feng[b], Yunfei Chen[b], Minfeng Wu[c], Yuanfang Zhang[b], Peibin Zhu[b], Wen Chen[b,*], Qihui Wu[a], Jianzhong Hao[d]

- A fast wavelet thresholding method based on signal estimation is proposed.
- It achieves both accurate threshold and real-time computation.
- Its denoising quality surpasses that of other methods.
- It can be applied to other wavelet transforms for denoising periodic signals.

Accurate wavelet thresholding method for ECG signals

Kaimin Yu[a], Lei Feng[b], Yunfei Chen[b], Minfeng Wu[c], Yuanfang Zhang[b], Peibin Zhu[b], Wen Chen[b,*], Qihui Wu[a], Jianzhong Hao[d]

School of Marine Equipment and Mechanical Engineering, Jimei University, Xiamen, 361021, Fujian, China

School of Ocean Information Engineering, Jimei University, Xiamen, 361021, Fujian, China

School of Electrical Engineering and Artificial Intelligence, Xiamen University Malaysia, Sepang, 43900, Malaysia

Institute of Infocomm Research (I^2R), Agency for Science, Technology and Research (A★STAR), 138632, Singapore

Abstract

Electrocardiogram (ECG) signals are a key element in the analysis and diagnosis of cardiovascular diseases. However, ECG signals are susceptible to interference from environmental noise, which affects the accuracy of diagnosis. Although the wavelet transform can denoise ECG signals, its efficacy is limited by the threshold value and threshold function. In this paper, an improved threshold wavelet function based on the tanh function is proposed on the basis of previously proposed thresholding methods based on signal estimation, especially the normalized autocorrelation function. Our experimental validation employs a variety of electrocardiogram (ECG) signals from different databases, each containing different types of noise such as additive Gaussian white noise (AWG), baseline drift, electrode motion, and muscle artifacts. The improved wavelet threshold function proposed in this paper performs well in removing AWG noise from ECG data. Notably, the maximum output signal-to-noise ratio of our improved threshold function exceeds that of existing methods at different input signal-to-noise ratios, while the minimum root-mean-square error is smaller. In addition, it also outperforms other methods in eliminating other real noise sources. This superiority stems from the fact that the improved wavelet threshold function is able to better remove the noise component and retain the signal portion, based on our precise distinction between AWG noise, which clearly deviates from the spectrum of the ECG signal, and real noise with similar spectral characteristics. Therefore, compared with the traditional threshold function method, our improved threshold function minimizes the change of signal components in the process of removing noise. Our proposed method effectively solves the pseudo-Gibbs effect and constant bias problems and enhances the visualization of denoised ECG signals during evaluation, thereby improving diagnostic accuracy.

Keywords: Wavelet transform, Biomedical analytical methods, Autocorrelation, Electrocardiography

1. Introduction

Cardiovascular disease stands as a leading cause of global mortality. Daily observation of vital sign signals, particularly electrocardiogram (ECG) signals, is instrumental in comprehending the occurrence, progression, and regression of this disease, forming the basis for prevention, diagnosis, treatment, and care [1–8]. However, signals captured by flexible and wearable sensors are vulnerable to interference from various noise and artifacts, including power line interference, electrode contact noise, baseline wander or shift, motion artifacts, electromyographic noise, instrumentation noise, and electrosurgical noise. Therefore, pre-processing or noise filtering is essential before accurately examining cardiac signal features [9–13], as it directly impacts the sensing system's performance. Currently, a range of noise removal techniques are available to sup-

*Corresponding author at: 185, Yinjiang Road, Jimei District, Xiamen City, Fujian 361021, China.

Email address: 2020610000040@jmu.edu.cn (Wen Chen[b,*])

press noise and artifacts in ECG signals, including digital filtering, adaptive noise reduction, wavelet transform, empirical mode decomposition, neural network-based methods, and hybrid methods [14–21]. Among these, wavelet transform stands out as one of the best denoising methods for non-stationary biomedical signals, widely used in image, sound, video, and mechanical processing fields [22–24]. In recent years, various wavelet transform methods have been developed to enhance the denoising of cardiac signals. Some of these methods involve improved wavelet transforms [25–29], such as Spcshrink of discrete wavelet transform (DWT), stationary wavelet transform (SWT), stationary wavelet packet transform (SWPT), dual-tree complex wavelet transform (DTCWT), double-density complex (DDC) DWT , and stationary bionic wavelet transform (SBWT). Others combine wavelet transforms with conventional methods [30–34], such as modified median filter, ensemble empirical mode decomposition (EEMD), local means filter, variational modal decomposition in addition to wavelet transform. Furthermore, some methods integrate wavelet transform with artificial intelligent (AI) [35–40], such as deep belief network fusion extreme learning machine (DBN-ELM), machine learning, deep learning. Certain approaches combine multiple methods mentioned above. The combination with wavelet transform and other methods is executed in two ways: first, by conducting traditional and/or AI processing followed by wavelet filtering, or vice versa; second, by enhance the accuracy of the wavelet thresholding using traditional and/or AI methods. Regardless of the denoising method or combination employed, the wavelet threshold plays a crucial role in the denoising results. Despite the advancements in denoising techniques, existing wavelet thresholding methods encounter challenges accurately determining thresholds for ECG signals with complex noise distributions and signal characteristics [41–48]. Most traditional wavelet thresholding methods are based on noise level estimation or wavelet coefficient characteristic estimation, such as noise variance, median absolute deviation, and singular value decomposition. Given that the noise spectrum may closely resemble the signal spectrum, accurately determining the threshold in practice is difficult, even after fine parameter adjustment. Other methods based on artificial intelligence algorithms may obtain relatively accurate thresholds, but demand extensive data training and currently are not applicable to real-time applications of heartbeat signal denoising.

This paper proposes a thresholding method for obtaining accurate wavelet thresholds in real time based on signal estimation, specifically the normalized autocorrelation function (ACF), instead of noise estimation, without the need for complex parameter tuning or extensive data training. Firstly, we introduce a normalized ACF-based wavelet thresholding method and its fast search algorithm. Secondly, we validate the proposed method by comparing its denoising results with those of other existing wavelet thresholding methods for various ECG signals with different types of noises, including additive white Gaussian (AWG) noise, baseline wandering noise, electrode motion noise, and muscle artifact noise. Furthermore, we verify this method by denoising measured ECG signals. Finally, we summarize the potential applications of the proposed method and outline future research directions.

2. Adaptive normalized ACF-based thresholding method

2.1. Accurate thresholding based on autocorrelation

To achieve accurate wavelet thresholds, we propose a wavelet thresholding method based on normalized ACF. For a short-term signal x, its autocorrelation function can be expressed as:

$$ACF(k) = \sum_{n=0}^{N-k-1} x(n)x_(n+k), \tag{1}$$

where N represents the signal length, n denotes the serial number of signal, k indicates the delay amount. If the signal is periodic, its autocorrelation function also exhibits the same periodicity. For instance, the 109 ECG signal from the MIT-BIH arrhythmia database [50], as depicted in Fig. 1(a), demonstrates the same periodicity as its non-zero-order periodic peak (NZOPP) of normalized ACF curve (red asterisk), illustrated in Fig. 1(b). The ACF of signal significantly differs from that of AWG noise with 5dB, as depicted in Figs. 1(c) and (d). This distinction arises from the clear correlation present in ECG signals, while noise lacks such correlation. When noise is added to the 109 ECG signal, the NZOPP of the normalized ACF decreases from 0.7183 to 0.5375, as illustrated in Figs. 1(e) and (f). Additionally, when AWG noise is continuously added to the

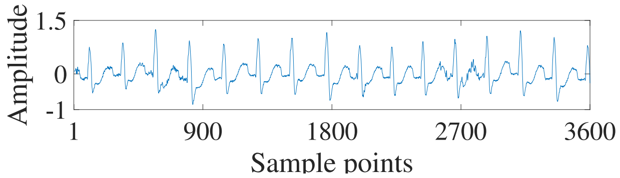

(a) Clean ECG signal.

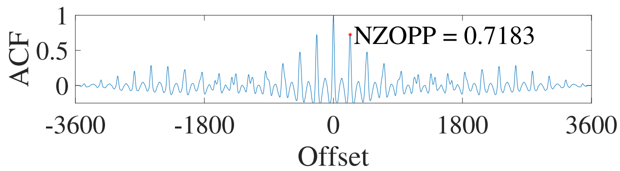

(b) Normalized ACF of clean ECG signal with NZOPP.

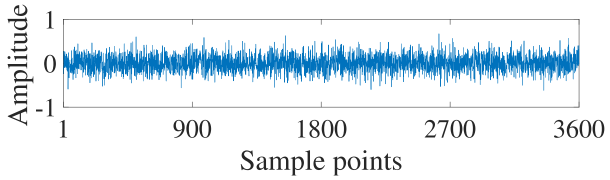

(c) White Gaussian noise.

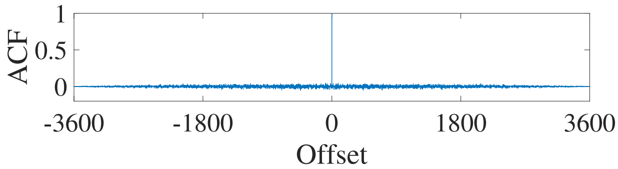

(d) Normalized ACF of white Guassian noise.

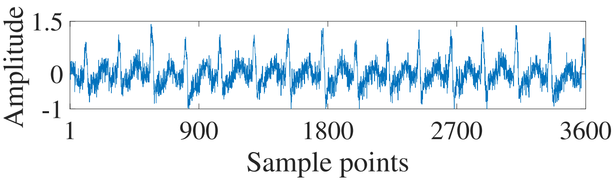

(e) ECG signal with white Gaussian noise.

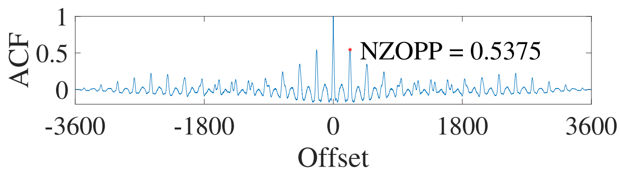

(f) Normalized ACF of noisy ECG signal with NZOPP.

Figure 1: Different signals and their autocorrelation functions. (a) Clean electrocardiogram signal and its (b) autocorrelation function; (c) Additive Gaussian white noise and its autocorrelation function; (e) Noisy electrocardiogram signal and its autocorrelation function

109 ECG signal from -30 dB to 30 dB, the NZOPP exhibits a monotonic, as shown in Fig. 2. Therefore, similar to the sig-

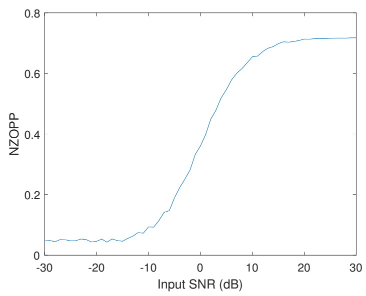

Figure 2: Relationship between NZOPP value and Input SNR.

nal-to-noise ratio (SNR) and structural similarity (SSIM), the NZOPP of normalized ACF can be utilized to access denoising quality and determine the accuracy threshold. Recently, the NZOPP has been successfully utilized to optimize non-local mean filtering parameters and evaluate the denoising quality of different image filters [51; 52]. It essentially evaluate the denoising quality based on signal characteristics instead of noise level. Traditionally, this method has proven to be a reliable tool for diagnosing mechanics faults, identifying pipeline leakage, recognizing cycle image textures, and so on [53–58].

The traditional thresholding method is typically based on noise estimation, for example, Universal threshold given by,

$$\lambda = \sigma\sqrt{2\ln N} \tag{2}$$

where λ represents the threshold value, N denotes the signal length, σ is the noise standard deviation. Subsequently, various studies have proposed enhancements based on this threshold, including formal improvements, and advancements in noise standard deviation estimation methods. However, as it is still relies on noise estimate that may not be accurately obtained in practice, conventional thresholding methods may not yield accurate wavelet thresholds. Furthermore, in addition to the wavelet thresholding method, the choice of threshold function also impacts the denoising outcome, with soft and hard threshold functions being commonly used.

$$\omega_\lambda = \begin{cases} \omega_i, & |\omega_i \geq \lambda, \\ 0, & |\omega_i| < \lambda, \end{cases} \tag{3}$$

$$\omega_\lambda = \begin{cases} \mathrm{sign}(\omega_i)(|\omega_i| - \lambda), & |\omega_i| \geq \lambda, \\ 0, & |\omega_i| < \lambda, \end{cases} \tag{4}$$

where ω_i is the wavelet coefficient, sign $(\cdot)$ is the signum function. Generally, SNR and root-mean-square error (RMSE) are used to evaluate the denoising quality.

$$\mathrm{SNR} = 10\log_{10}\left\{\sum_{n=1}^{N}\frac{y(n)^2}{[x(n)-y(n)]^2}\right\}, \tag{5}$$

$$\mathrm{RMSE} = \frac{1}{N}\sqrt{\sum_{n=1}^{N}[x(n)-y(n)]^2}, \tag{6}$$

where $x(n)$ and $y(n)$ are the clean signal and the denoised signal, respectively. However, clean signals are usually unavailable in practice.

2.2. Fast threshold calculation algorithm

To expedite threshold querying, an algorithm has been developed to determine the optimal threshold, as illustrated in Fig. 3.

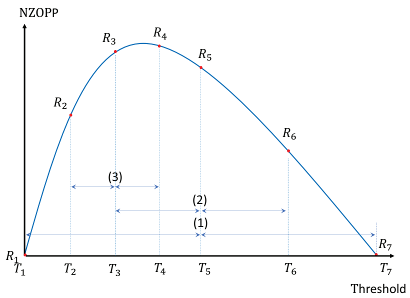

Figure 3: Flowchart of fast threshold querying algorithm.

(1) Denoise the given noisy signal using predefined initial threshold values $[T_1, T_2, T_3]$ to obtain three denoised signals;

(2) Calculate the maximum NZOPP for each denoised signal $[R_1, R_2, R_3]$ and identify the maximum R_2;

(3) Interpolate on both sides of T_2 to generate a new threshold sequence $[T_1, (T_1 + T_2)/2, T_2, (T_2 + T_3)/2, T_3]$, i.e., $[T_1, T_2, T_3, T_4, T_5]$;

(4) Apply the threshold sequence $[T_1, T_2, T_3, T_4, T_5]$ to denoise the noisy signal and calculate the maximum NZOPP for the denoised signals $[R_1, R_2, R_3, R_4, R_5]$;

(5) Identify the largest R_3 from $[R_1, R_2, R_3, R_4, R_5]$ and its corresponding threshold T_3 ;

(6) Interpolate on both sides of T_3 to obtain a new threshold sequence $[T_1,\ T_2,\ (T_2 + T_3)/2,\ T_3,\ (T_3 + T_4)/2,\ T_4,\ T_5]$, i.e., $[T_1, T_2, T_3, T_4, T_5, T_6, T_7]$;

(7) Check if the difference between adjacent thresholds is less than 10^{-10}, i.e., $|T_3 - T_4| < 10^{-10}$;

(8) Repeat steps (4) to (7) until condition (7) is satisfied, then output the optimal threshold T_i corresponding to the maximum NZOPP (R_i).

In summary, the thresholds are continuously interpolated to find the maximum NZOPP that corresponds to the optimal wavelet threshold.

3. Numerical comparisons

To validate the proposed ACF-based adaptive thresholding method, we applied it to denoise several ECG signals (Fig. 4) with various noise disturbances (Fig. 5). We compared the denoising results with those obtained using existing popular thresholding methods such as Universal, Heursure, Minimax, and Bayes. Figures 4(a) and (c) depicted ECG signals 109 and 233 from the MIT-BIH Arrhythmia Database [50]. Figure 4(a) shows the ECG signals in the presence of first-degree atrioventricular(AV) block and multiform Premature Ventricular Contractions (PVCs), while Fig. 4(c) displays only the ECG signal with multiform PVCs. Figures 4(e) and (g) represent cu07 and cu11 ECG signals of human subjects who experienced episodes of sustained ventricular tachycardia, ventricular flutter, and ventricular fibrillation from the Creighton University Ventricular Tachyarrhythmia Database [59]. Figures 4(i) and (k) show the s00161rem and s00261rem ECG signals of myocardial infarction in female and male subjects from the PTB Diagnostic ECG Database [60], respectively. The corresponding spectra of the above-mentioned ECG signals are shown in Figs. 4(b), (d), (f), (h), (j), and (l) respectively. Interference to multiple ECG signals includes baseline wander,electrode motion artifact, and muscle artifacts besides of AWG noise, which comes from the MIT-BIH noise stress test database [61], as shown in Fig. 5. Their corresponding spectra are displayed in Fig. 5(b), (d), (f), and (h) respectively. The experiments utilized the soft thresholding function and db3 wavelet basis. This test was conducted

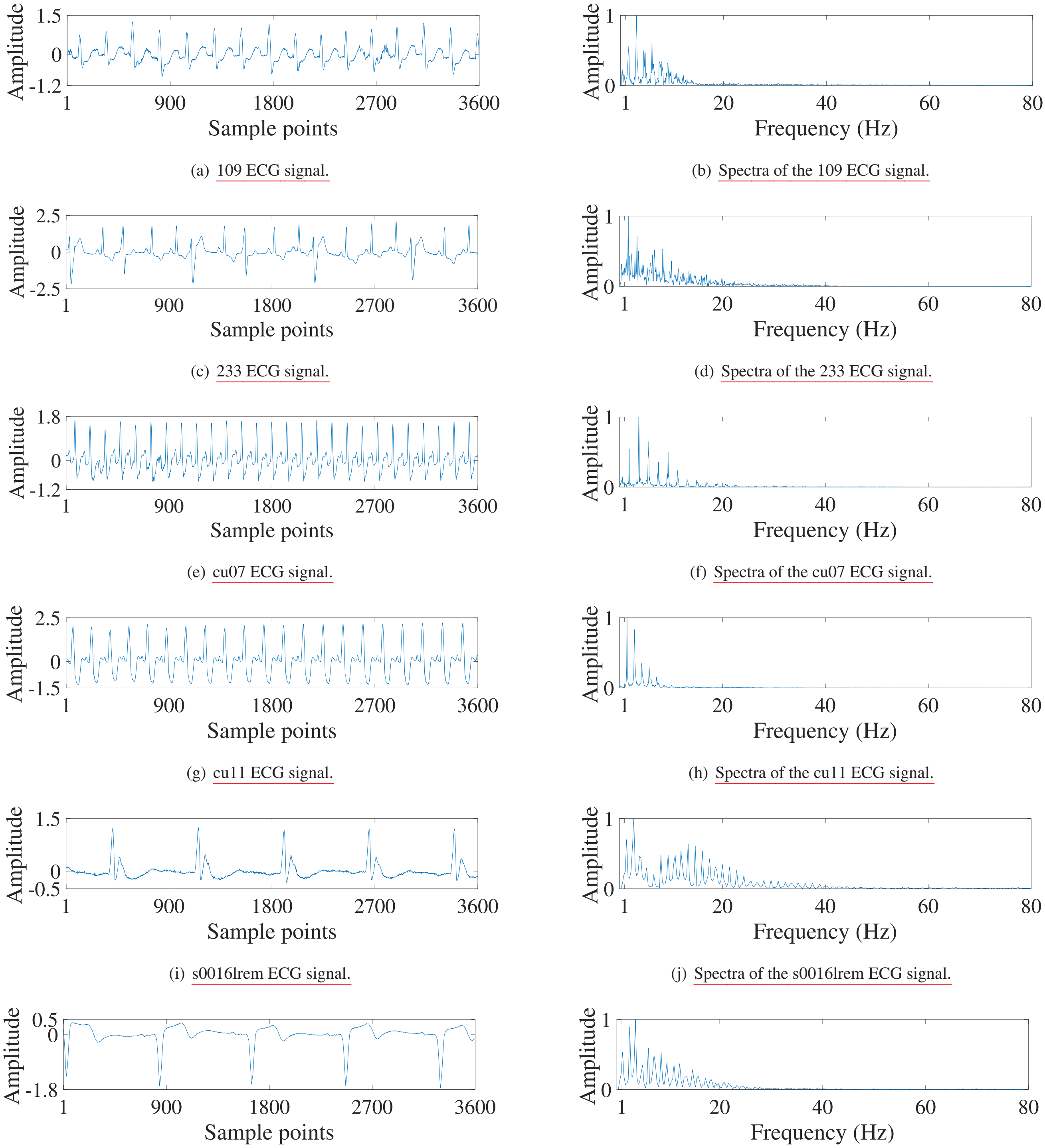

(a) 109 ECG signal.

(b) Spectra of the 109 ECG signal.

(c) 233 ECG signal.

(d) Spectra of the 233 ECG signal.

(e) cu07 ECG signal.

(f) Spectra of the cu07 ECG signal.

(g) cu11 ECG signal.

(h) Spectra of the cu11 ECG signal.

(i) s0016lrem ECG signal.

(j) Spectra of the s0016lrem ECG signal.

(k) s0026lrem ECG signal.

(l) Spectra of the s0026lrem ECG signal.

Figure 4: Different signals and their Spectra. (a) 109 ECG signal and its (b) Spectra; (c) 233 ECG signal and its (d) Spectra; (e) cu07 ECG signal and its (f) Spectra; (g) cu11 ECG signal and its (h) Spectra; (i) s00161rem ECG signal and its (j) Spectra; (k) s00261rem ECG signal and its (l) Spectra;

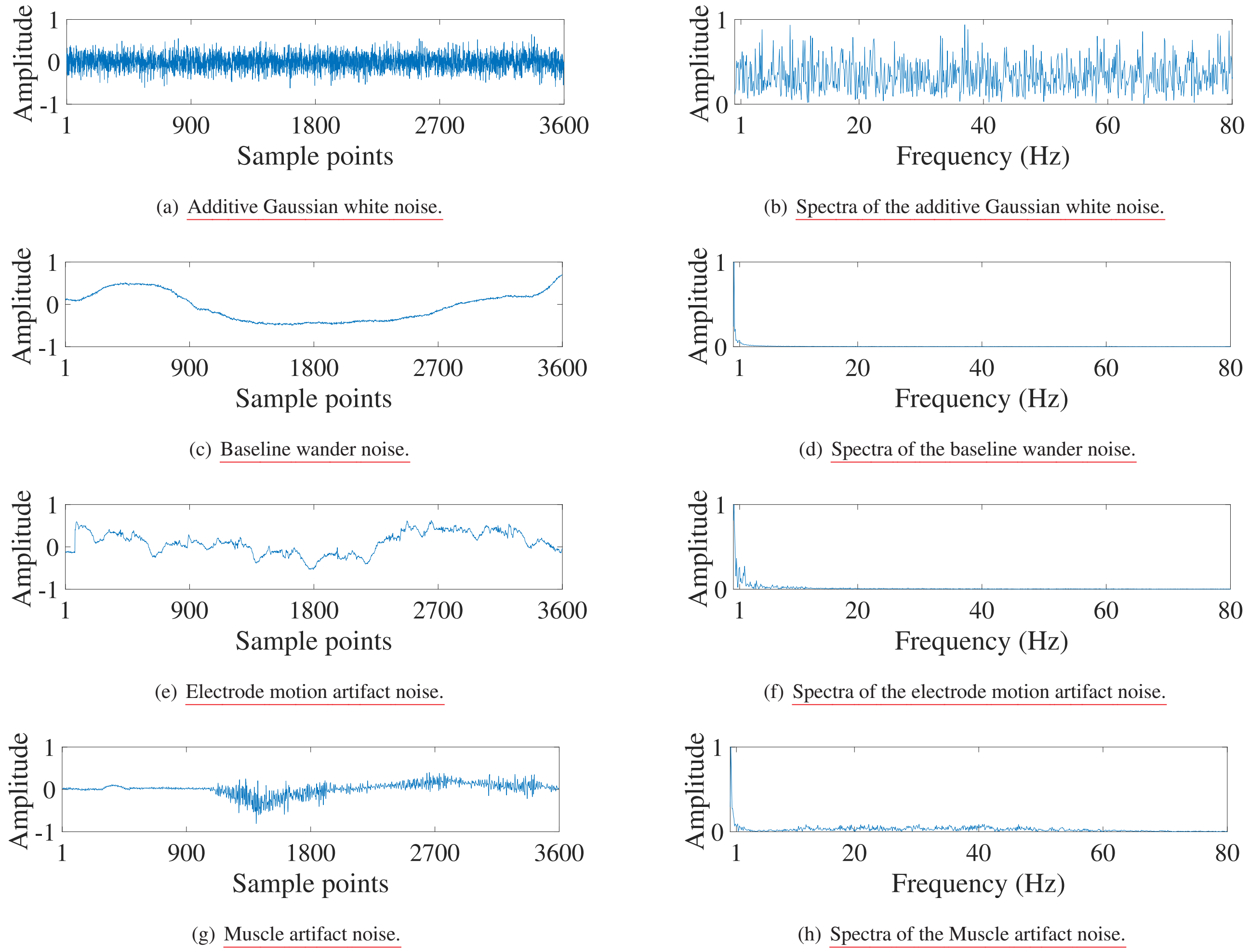

Figure 5: Different noises and their Spectra. (a) Additive Gaussian white noise and its (b) Spectra; (c) Baseline wander noise and its (d) Spectra; (e) Electrode motion artifact noise and its (f) Spectra; (g) Muscle artifact noise and its (h) Spectra;

using MATLAB R2023a software on a 64 bit Windows 11 operating system. The computer used for the test is equipped with a 2.70 GHz Intel Core i7 processor and 16 GB of RAM.

3.1. *ECG signals with additive white Gaussian noise*

The 109 ECG signals from the MIT-BIH Arrhythmia Database, contaminated by -10 to 30 dB input AWG noise, were denoised by using different thresholding methods. Figure 6 illustrates the variation in output SNR with the wavelet decomposition layer. It evdient that the proposed method's output SNR at the optimal decomposition layer outperforms that of the other thresholding methods across a wide input SNR range from -10 dB to 30 dB, except for input SNR of 10dB to 20dB, where it is slightly lower than that of the Bayes thresholding method. Figure 7 demonstrates that the RMSE is lower than that of other methods across the wide input SNR range. Both the larger SNR and smaller RMSE indicate that the proposed method achieves more accurate wavelet threshold than the other thresholding methods.

Figure 8 provides a visual comparison of the signals denoised using different thresholding methods. The noisy signal was obtained by adding 5 dB of AWG noise to the 109 ECG signal, as depicted in Fig. 8(a). The denoising signals at the optimal decomposition layer obtained using different thresholding methods are presented in Figs. (b)-(f). Figure 8(b) illustrates that the ACF thresholding method effectively removes noise while preserving the components of the ECG signal more comprehensively. In contrast, Figs. 8(c)-(e) exhibit significant residual noise, indicating that other methods (e.g., Universal thresh-

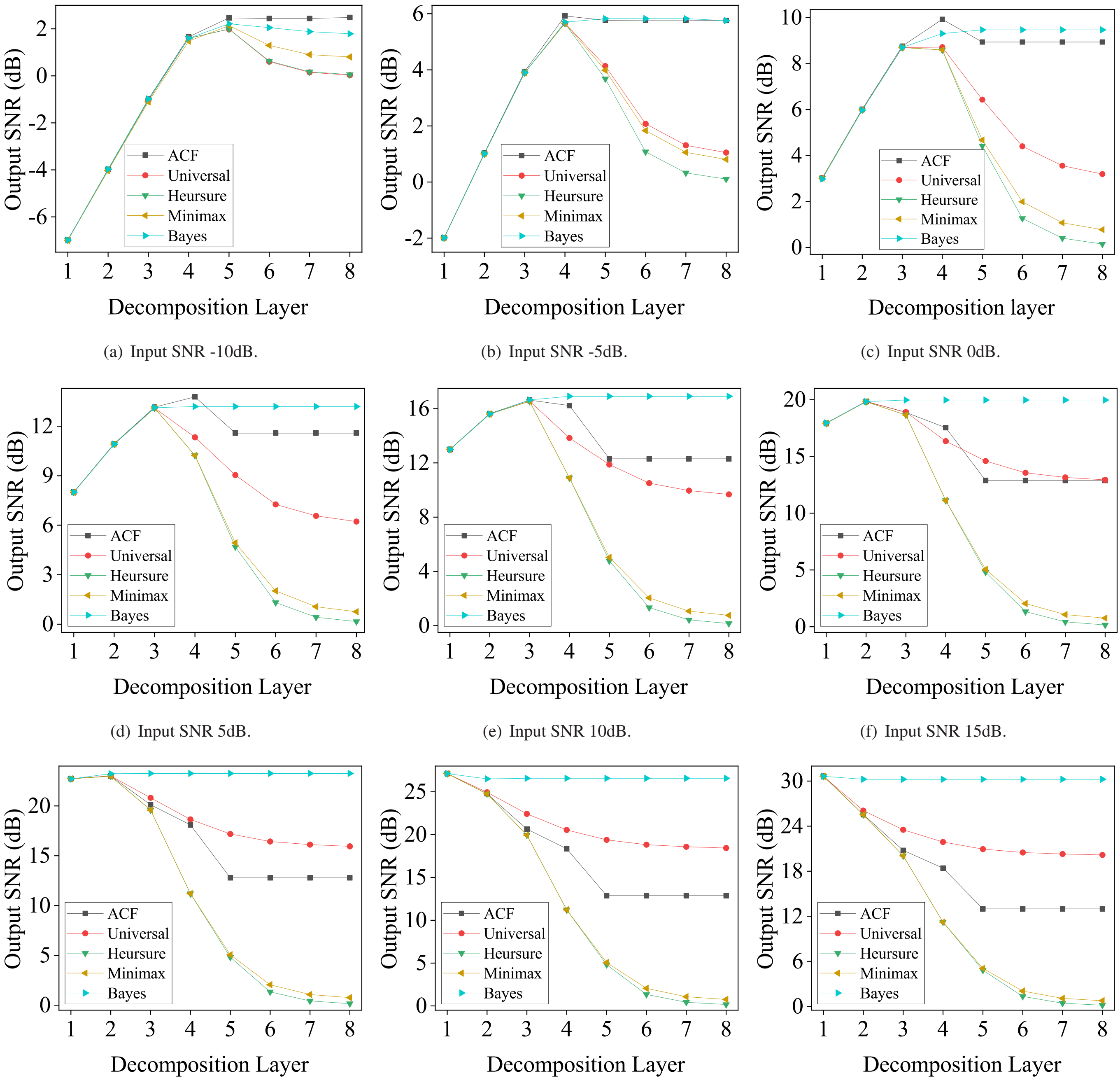

(a) Input SNR -10dB. (b) Input SNR -5dB. (c) Input SNR 0dB.

(d) Input SNR 5dB. (e) Input SNR 10dB. (f) Input SNR 15dB.

(g) Input SNR 20dB. (h) Input SNR 25dB. (i) Input SNR 30dB.

Figure 6: Comparison of output SNR of denoised signals with the input SNR varying from -10 dB to 30 dB using different wavelet thresholding methods.

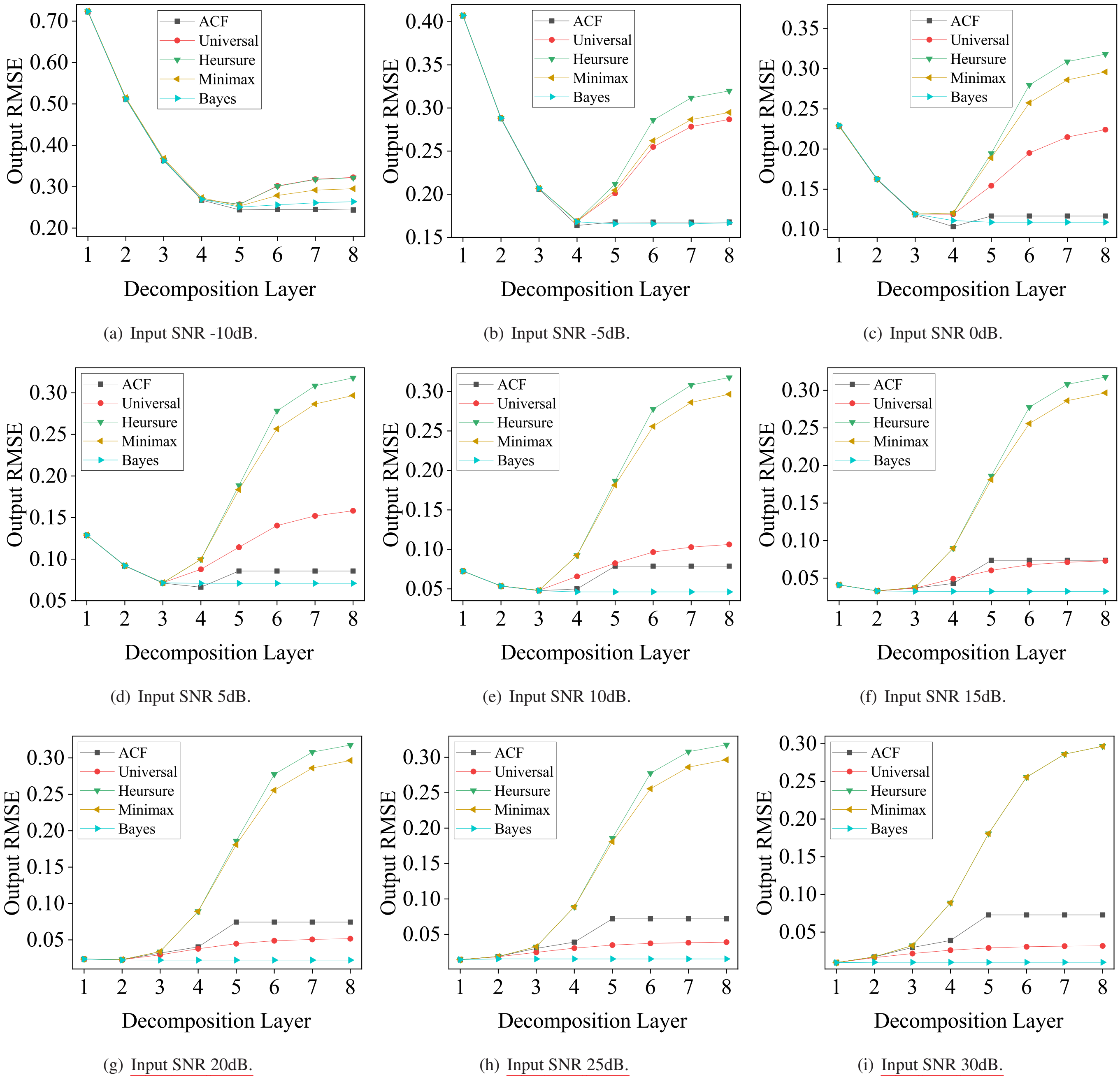

(a) Input SNR -10dB. (b) Input SNR -5dB. (c) Input SNR 0dB.

(d) Input SNR 5dB. (e) Input SNR 10dB. (f) Input SNR 15dB.

(g) Input SNR 20dB. (h) Input SNR 25dB. (i) Input SNR 30dB.

Figure 7: Comparison of output RMSE of denoised signals with the input SNR varying from -10dB to 30 dB using different wavelet thresholding methods.

Table 1: **Comparison of the optimal output SNRs and RMSEs of 109 ECG signal with AWG noise denoised by different thresholding methods.**

Input	ACF		Universal		Heursure		Minimax		Bayes	
SNR	SNR	RMSE	SNR	RMSE	SNR	RMSE	SNR	RMSE	SNR	RMSE
-10	**2.4641**	**0.2441**	1.9856	0.2577	1.5968	0.2575	1.4751	0.2533	2.2149	0.2510
-5	**5.9211**	**0.1638**	5.6653	0.1687	5.6569	0.1689	5.6611	0.1688	5.8251	0.1656
0	**9.9280**	**0.1033**	8.7146	0.1187	8.5956	0.1203	8.5956	0.1203	9.4687	0.1089
5	**13.7823**	**0.0662**	13.1024	0.0716	13.1019	0.0716	13.1019	0.0716	13.1961	0.07089
10	16.6296	0.0477	16.5601	0.048	16.5390	0.0482	16.5390	0.0482	**16.9093**	**0.0463**
15	19.8481	0.0329	19.8215	0.0330	19.8207	0.0330	19.8207	0.0330	**19.9664**	**0.0325**
20	23.0055	0.0229	23.0044	0.0229	22.9833	0.0230	22.9833	0.0230	**23.2571**	**0.0223**
25	**27.1260**	**0.0143**	27.1052	0.0143	27.1052	0.0143	27.1052	0.0143	27.1189	0.0143
30	**30.6670**	**0.0095**	30.6282	0.0095	30.6282	0.0095	30.6282	0.0095	30.6435	0.0095

olding, Heursure thresholding, and Minimax thresholding) have poorer threshold accuracy, resulting in inferior noise reduction. Bayes thresholding achieves a denoised signal comparable to our method, as shown in Fig. 8(f). This visual evidence aligns with the results shown in Fig. 6(d), further affirming the superiority of our method.

To assess the generality of the proposed thresholding method, we compared the output SNRs and RMSEs of different thresholding methods for denoising multiple ECG signals (as shown in Fig. 4) with input SNR levels ranging from -10 dB to 10 dB, as listed in Table 2. Each output is the average result of 100 denoisings to mitigate the impact of different AWG noise distributions. It is evident that the proposed method significantly outperforms the other methods in the most cases (highlighted in bold in the first two columns).

It is noteworthy that only 79 fast threshold iterations are required to attain a threshold accuracy of 10^{-10}, indicating that the algorithm is computationally efficient. However, such a high thresholding accuracy is unnecessary since proposed threshold accuracy higher than 10^{-2} cannot significantly enhance the output SNR. To assess the computational cost of different thresholding methods, we employed four wavelet decomposition layers to denoise the 109 ECG signal with the 5 dB AWG noise. Table 3 demonstrates that the proposed method's time consumption (0.0846 seconds) is much higher than that of other methods, indicating that the proposed method is more complex. Nevertheless, it achieves the highest output SNR (13.7062 dB) among the compared methods.

3.2. *ECG signals with other types of noise*

To validate the efficacy of the proposed thresholding method on different types of noise, we applied the method to denoise ECG signals contaminated by the real noise and compared the results with those obtained using other methods. The denoising effect of various thresholding methods at the optimal decomposition layer was evaluated by SNR_{imp} (= output SNR - input SNR) and RMSE, as detailed in Tables 4, 5, and 6. The SNR_{imp} (highlighted in bold in the first column) of our proposed method is significantly higher than that of the other methods, and the RMSE (highlighted in bold in the second column) is notably smaller, regardless of the type of noise added to the ECG signal. The denoising effect of the proposed method on ECG signals containing actual noise surpasses that of ECG signals containing AWG noise, as the spectrum of real noise more closely

Table 2: **Comparison of the optimal output SNRs and RMSEs of multiple ECG signals with AWG noise denoised by different thresholding methods.**

Record	Input	ACF		Universal		Heursure		Minimax		Bayes	
	SNR	SNR	RMSE	SNR	RMSE	SNR	RMSE	SNR	RMSE	SNR	RMSE
233	-10	**2.1795**	**0.4216**	1.4962	0.4548	1.6952	0.4446	0.1075	0.5337	1.7627	0.4412
	-5	**6.0286**	**0.2705**	4.9495	0.3056	4.9380	0.3060	5.1784	0.2978	5.2043	0.2969
	0	**9.9785**	**0.1716**	8.4455	0.2043	8.4448	0.2044	8.4450	0.2043	9.2270	0.1868
	5	**13.7469**	**0.1110**	12.4765	0.1285	12.4421	0.1290	12.4421	0.1290	12.8336	0.1233
	10	**17.5433**	**0.0718**	15.8176	0.0874	15.8175	0.0874	15.8175	0.0874	16.7815	0.0783
cu07	-10	**1.2520**	**0.4234**	0.8520	0.4431	0.8093	0.4453	-0.1812	0.4990	0.8574	0.4428
	-5	**4.9117**	**0.2779**	4.0448	0.3067	4.0241	0.3075	4.1949	0.3015	4.3560	0.2960
	0	**8.7795**	**0.1779**	8.0935	0.1925	8.0918	0.1925	8.0919	0.1925	8.1349	0.1916
	5	**12.5141**	**0.1157**	11.6137	0.1283	11.5852	0.1287	11.5852	0.1287	12.0194	0.1225
	10	**16.0944**	**0.0766**	15.5337	0.0817	15.5335	0.0817	15.5335	0.0817	15.7623	0.0796
cu11	-10	**2.9720**	**0.5934**	2.5829	0.6196	0.5067	0.7869	-2.9986	1.1778	2.6448	0.6153
	-5	**6.9370**	**0.3756**	6.3268	0.4028	6.2832	0.4048	5.1925	0.4589	6.0658	0.4151
	0	**10.7203**	**0.2428**	10.0121	0.2634	10.0078	0.2635	10.0434	0.2624	10.0769	0.2614
	5	**14.6176**	**0.1550**	13.7088	0.1721	13.7087	0.1721	13.7087	0.1721	13.7089	0.1721
	10	**18.5062**	**0.0990**	18.1257	0.1035	18.1251	0.1035	18.1251	0.1035	18.3577	0.1008
s0016lrem	-10	**4.7826**	**0.1294**	2.4948	0.1678	2.3723	0.1701	2.5990	0.1658	3.1927	0.1549
	-5	**8.7100**	**0.0821**	6.5475	0.1053	6.5456	0.1053	6.5456	0.1053	7.1272	0.0985
	0	**12.4922**	**0.0531**	10.5934	0.0660	10.4444	0.0672	10.4444	0.0672	11.2727	0.0611
	5	**16.0941**	**0.0351**	14.2869	0.0431	14.2869	0.0431	13.6549	0.0464	15.0794	0.0394
	10	**19.3172**	**0.0242**	17.9429	0.0283	17.9379	0.0283	17.9379	0.0283	18.4910	0.0266
s0026lrem	-10	**4.9041**	**0.1856**	4.3612	0.1953	4.3618	0.1953	4.2974	0.1967	4.7646	0.1865
	-5	**9.0168**	**0.1143**	8.1686	0.1259	8.0994	0.1269	8.1331	0.1264	8.5822	0.1202
	0	**13.3787**	**0.0692**	11.7418	0.0835	11.7409	0.0835	11.7409	0.0835	12.5962	0.0757
	5	**17.1774**	**0.0446**	15.9396	0.0515	15.9096	0.0516	15.9096	0.0516	16.5062	0.0482
	10	20.2133	0.0315	19.6523	0.0336	19.1891	0.0354	19.1891	0.0354	**20.2574**	**0.0313**

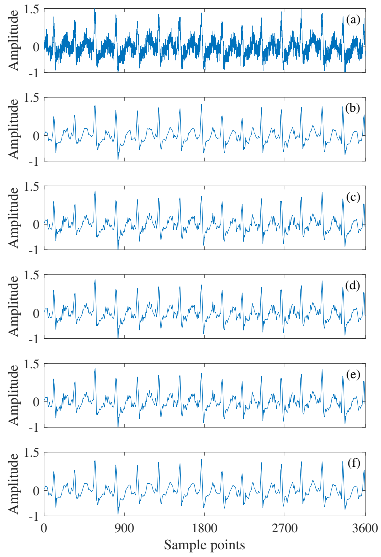

Figure 8: Comparison of denoising results for (a) the 109 ECG signal from MIT-BIH database corrupted by 5 dB input SNR WGN using different thresholding methods, including (b) ACF, (c) Universal, (d) Heursure, (e) Minimax, and (f) Bayes.

Table 3: **Computational cost comparison.**

Methods	ACF	Universal	Heursure	Minimax	Bayes
Cost (s)	0.0846	0.0055	0.0075	0.0052	0.0106
SNR (dB)	13.7062	13.0405	13.0036	13.0036	13.1238

resembles the signal spectrum than that of AWG noise. When there is a significant difference between the noise spectrum and the signal spectrum, traditional thresholding methods based on noise estimation can obtain accurate thresholds and effectively remove noise from signal. However, if the noise spectrum and signal spectrum are similar, traditional methods may struggle to obtain accurate thresholds, whereas our proposed method can still achieve accurate thresholds and effectively remove noise.

3.3. Measured ECG signal

To validate the practicality of the proposed method, we applied it to denoise the III-lead signals in real 12-lead ECG signals with a frequency of 500 Hz using different thresholding methods, and compared their denoising signals. As the noise distribution in the real signal is unknown, selecting the appropriate decomposition layer is crucial to achieve the maximum output SNR. Our experiments revealed that a three-layer wavelet decomposition resulted in a significant amount of residual noise, while a five-layer decomposition led to the loss of signal components (refer to Supplementary Material for detailed description). Therefore, a four-layer decomposition was found to yield the best denoised signal.

Figure 9 (a) illustrates the measured ECG signal affected by noise. The denoising results of the real ECG signal using different thresholding methods are depicted in Figs. 9 (b)-(f). Neither Universal and Bayes thresholding effectively eliminated noise, as shown in Figs. 9 (c) and (f), which is consistent with the previous findings [43]. While the Bayes thresholding method performs well on ECG signals from MIT-BIH database, it struggled when applied to real signals due to its reliance on a priori noise distributions. The denoising results obtained by Heursure and Minimax thresholding methods, as shown in Figs. 9 (d) and (e), revealed that they remove the noise at the expense of severe loss of signal components. Therefore, it is evident that the proposed method not only maximizes noise suppression but also effectively preserves the signal components.

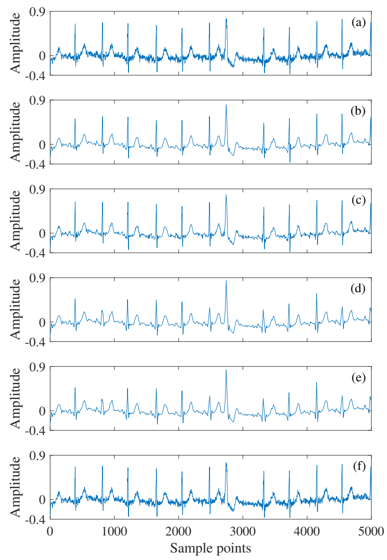

Figure 9: Visual comparison of the denoising results of 4-layer decomposition of (a) the measured ECG signal using different thresholding methods, including (b) ACF, (c) Universal, (d) Heursure, (e) Minimax, and (f) Bayes.

Table 4: **Comparison of SNRs improvement and RMSEs of multiple ECG signals with baseline wander noise denoised by different thresholding methods.**

Record	ACF		Universal		Heursure		Minimax		Bayes	
	SNR_{imp}	RMSE	SNR_{imp}	RMSE	SNR_{imp}	RMSE	SNR_{imp}	RMSE	SNR_{imp}	RMSE
109	**0.70471**	**0.31537**	0.00827	0.34170	-0.00053	0.34205	-0.00053	0.34205	-0.00052	0.34205
233	**3.03255**	**0.24123**	0.02584	0.34101	-0.00017	0.34203	-0.00017	0.34203	-0.00012	0.34203
cu07	**1.2073**	**0.29764**	-0.00093	0.34206	-0.00093	0.34206	-0.00093	0.34206	-0.00063	0.34205
cu11	**1.7641**	**0.27915**	0.00030	0.34201	0.00030	0.34201	0.00030	0.34201	0.00031	0.34201
s0016lrem	**2.66781**	**0.25157**	0.03139	0.34079	0.52615	0.32192	0.33740	0.32899	0.00030	0.34201
s0026lrem	**4.83571**	**0.19601**	0.02787	0.34093	0.00163	0.34196	0.00163	0.34196	0.00079	0.34120

Table 5: **Comparison of SNRs improvement and RMSEs of multiple ECG signals with electrode motion noise denoised by different thresholding methods.**

Record	ACF		Universal		Heursure		Minimax		Bayes	
	SNR_{imp}	RMSE	SNR_{imp}	RMSE	SNR_{imp}	RMSE	SNR_{imp}	RMSE	SNR_{imp}	RMSE
109	**1.49446**	**0.23224**	0.11760	0.27025	0.000028	0.27583	0.000028	0.27583	-0.000134	0.27584
233	**4.39780**	**0.16625**	0.13130	0.27170	0.00092	0.27581	0.00092	0.27581	0.00074	0.27582
cu07	**0.96397**	**0.24686**	0.0877	0.27307	-0.00024	0.27584	-0.00024	0.27584	-0.0000053	0.27584
cu11	**2.56726**	**0.20526**	0.08659	0.27310	0.00150	0.27579	0.00150	0.27579	0.00121	0.27580
s0016lrem	**4.05475**	**0.17295**	0.15989	0.27081	0.78610	0.25197	0.72930	0.25363	0.00160	0.27579
s0026lrem	**5.21242**	**0.15137**	0.10578	0.27250	0.013750	0.27540	0.013750	0.27540	0.00158	0.27579

Table 6: **Comparison of SNRs improvement and RMSEs of multiple ECG signals with muscle artifact noise denoised by different thresholding methods**

Record	ACF		Universal		Heursure		Minimax		Bayes	
	SNR_{imp}	RMSE	SNR_{imp}	RMSE	SNR_{imp}	RMSE	SNR_{imp}	RMSE	SNR_{imp}	RMSE
109	**0.93214**	**0.12569**	0.80942	0.12748	0.86735	0.12663	0.86735	0.12663	0.02486	0.13953
233	**1.16789**	**0.12233**	0.71803	0.12883	0.29556	0.13525	0.29556	0.13525	0.02469	0.13954
cu07	**0.63469**	**0.13007**	0.44281	0.13298	0.21910	0.13645	0.21910	0.13645	0.02271	0.13957
cu11	**1.94719**	**0.11183**	0.66136	0.12967	0.59893	0.13061	0.59893	0.13061	0.02479	0.13953
s0016lrem	**7.06482**	**0.06204**	0.89813	0.12619	1.14746	0.12262	1.14746	0.12262	0.02590	0.13952
s0026lrem	**6.08226**	**0.06947**	0.83861	0.12706	1.36534	0.11958	1.36534	0.11958	0.02216	0.13958

4. Conclusion

A fast wavelet thresholding method based on signal estimation, i.e., ACF, is proposed instead of traditional noise estimation to obtain accurate thresholds in real time. It utilizes the fact that noise has no autocorrelation while signal has correlation to accurately estimate signal, i.e., non-zero order periodic peaks of periodic signals, achieving a significant improvement in the output SNR of periodic signals at low computation cost. The method is validated by denoising multiple ECG signals containing different types of noise, including AWG noise, baseline wander noise, electrode motion noise, and muscle artifact noise.

- The proposed ACF threshold method is only slightly superior to other methods in removing AWG noise from multiple electrocardiogram signals, as both the traditional method and the proposed threshold method can accurately estimate AWG noise with significant spectra differences from the heartbeat signal.
- It far surpasses all other methods in removing real noise such as baseline wander noise, electrode motion noise, and muscle artifact noise, because traditional thresholding methods cannot accurately estimate noise whose spectrum resembles to the spectrum of the heartbeat signal, whereas the proposed method can still accurately estimate the signal, in other words, can accurately estimate the noise.
- In addition, it is visually superior to other thresholding methods for denoising the measured ECG signal.

It overcomes both the inability of traditional thresholding methods to accurately estimate noise and the time consuming of AI-based thresholding methods. It is only suitable for wavelet threshold optimization of periodic signals due to its autocorrelation function. However, future research work can expand the application in determining precise thresholds for other wavelet transforms (such as SWT, SWPT, DTCWT, etc.), as well as the application in optimizing their threshold function, decomposition layer, and wavelet basis. This work not only improves the denoising results of wavelet, but also contributes to more accurately diagnosis cardiovascular diseases in the future.

Acknowledgements

This work was supported by the Educational and Scientific Research Projects for Young [JAT200236, JAT200289]; and the Natural Science Foundation of Fujian Science and Technology Plan under Grant [2022J01824, 2021J01866].

References

[1] G. Swapna, K.P. Soman, R. Vinayakumar, Diabetes detection using ECG signals: An overview, in: S. Dash, B.R. Acharya, M. Mittal, A. Abraham, A. Kelemen (Eds.), Deep learning techniques for biomedical and health informatics, Springer International Publishing, Cham, 2020: pp. 299–327. https://doi.org/10.1007/978-3-030-33966-1_14.

[2] J. Lin, R. Fu, X. Zhong, P. Yu, G. Tan, W. Li, H. Zhang, Y. Li, L. Zhou, C. Ning, Wearable sensors and devices for real-time cardiovascular disease monitoring, Cell Reports phys. sci. 2 (2021) 100541. https://doi.org/10.1016/j.xcrp.2021.100541.

[3] G. Cosoli, S. Spinsante, F. Scardulla, L. D'Acquisto, L. Scalise, Wireless ECG and cardiac monitoring systems: State of the art, available commercial devices and useful electronic components, Measurement 177 (2021) 109243. https://doi.org/10.1016/j.measurement.2021.109243.

[4] Y. Guo, X. Liu, S. Peng, X. Jiang, K. Xu, C. Chen, Z. Wang, C. Dai, A review of wearable and unobtrusive sensing technologies for chronic disease management, Comput. Biol. Med. 129 (2021) 104163. https://doi.org/10.1016/j.compbiomed.2020.104163.

[5] S. Dami, M. Yahaghizadeh, Predicting cardiovascular events with deep learning approach in the context of the internet of things, Neural Comput. Appl. 33 (2021) 7979–7996. https://doi.org/10.1007/s00521-020-05542-x.

[6] F. Santucci, D. Lo Presti, C. Massaroni, E. Schena, R. Setola, Precordial vibrations: A review of wearable systems, Signal processing techniques, and main applications, Sensors 22 (2022) 5805. https://doi.org/10.3390/s22155805.

[7] A. Rath, D. Mishra, G. Panda, S.C. Satapathy, An exhaustive review of machine and deep learning based diagnosis of heart diseases, Multimed Tools Appl. 81 (2022) 36069–36127. https://doi.org/10.1007/s11042-021-11259-3.

[8] S. Zhang, Q. Sun, L. Yao, A. Zhang, R. Zhang, Feature detection algorithm combined with machine learning applied to abnormal ECG diagnosis system, in: R. Kountchev, K. Nakamatsu, W. Wang, R. Kountcheva (Eds.), Proceedings of the world conference on intelligent and 3-D technologies (WCI3DT 2022), Springer Nature Singapore, Singapore, 2023: pp. 207–216. https://doi.org/10.1007/978-981-19-7184-6_17.

[9] S. Chatterjee, R.S. Thakur, R.N. Yadav, L. Gupta, D.K. Raghuvanshi, Review of noise removal techniques in ECG signals, IET Signal Process. 14 (2020) 569–590. https://doi.org/10.1049/iet-spr.2020.0104.

[10] F. Jiang, Y. Zhou, T. Ling, Y. Zhang, Z. Zhu, Recent research for unobtrusive atrial fibrillation detection methods based on cardiac dynamics signals: A survey, Sensors 21 (2021) 3814. https://doi.org/10.3390/s21113814.

[11] S.K. Saini, R. Gupta, Artificial intelligence methods for analysis of electrocardiogram signals for cardiac abnormalities: state-of-the-art and future challenges, Artif. Intell. Rev. 55 (2022) 1519–1565. https://doi.org/10.1007/s10462-021-09999-7.

[12] E.H. Houssein, I.E. Ibrahim, M. Hassaballah, Y.M. Wazery, Integration of machine learning and optimization techniques for cardiac health recognition, in: E.H. Houssein, M. Abd Elaziz, D. Oliva, L. Abualigah (Eds.), Integrating meta-heuristics and machine learning for real-world optimization Problems, Springer International Publishing, Cham, 2022: pp. 121–148. https://doi.org/10.1007/978-3-030-99079-4_6.

[13] I. El Boujnouni, H. Zili, A. Tali, T. Tali, Y. Laaziz, A wavelet-based capsule neural network for ECG biometric identification, Biomed. Signal Process. 76 (2022) 103692. https://doi.org/10.1016/j.bspc.2022.103692.

[14] P.M. Tripathi, A. Kumar, R. Komaragiri, M. Kumar, A review on computational methods for denoising and detecting ECG signals to detect cardiovascular diseases, Arch. Comput. Meth. Eng. 29 (2022) 1875–1914. https://doi.org/10.1007/s11831-021-09642-2.

[15] R. Martinek, M. Ladrova, M. Sidikova, R. Jaros, K. Behbehani, R. Kahankova, A. Kawala-Sterniuk, Advanced bioelectrical signal processing methods: Past, present and future approach—part I: Cardiac signals, Sensors 21 (2021) 5186. https://doi.org/10.3390/s21155186.

[16] R. Martinek, M. Ladrova, M. Sidikova, R. Jaros, K. Behbehani, R. Kahankova, A. Kawala-Sterniuk, Advanced bioelectrical signal processing methods: Past, present and future approach—part II: Brain signals, Sensors 21 (2021) 6343. https://doi.org/10.3390/s21196343.

[17] R. Martinek, M. Ladrova, M. Sidikova, R. Jaros, K. Behbehani, R. Kahankova, A. Kawala-Sterniuk, Advanced bioelectrical signal processing methods: Past, present, and future approach—part III: Other biosignals, Sensors 21 (2021) 6064. https://doi.org/10.3390/s21186064.

[18] P.D. Barua, E. Aydemir, S. Dogan, M.A. Kobat, F.B. Demir, M. Baygin, T. Tuncer, S.L. Oh, R.-S. Tan, U.R. Acharya, Multilevel hybrid accurate handcrafted model for myocardial infarction classification using ECG signals, Int. J. Mach. Learn. & Cyber. 14 (2023) 1651-1668. https://doi.org/10.1007/s13042-022-01718-0.

[19] A. Subasi, S. Dogan, T. Tuncer, A novel automated tower graph based ECG signal classification method with hexadecimal local adaptive binary pattern and deep learning, J. Ambient Intell Human Comput. 14 (2023) 711-725. https://doi.org/10.1007/s12652-021-03324-4.

[20] M.A. Kobat, O. Karaca, P.D. Barua, S. Dogan, PrismatoidPatNet54: An Accurate ECG Signal Classification Model Using Prismatoid Pattern-Based Learning Architecture, Symmetry. 13 (2021) 1914. https://doi.org/10.3390/sym13101914.

[21] F. Shi, A review of noise removal techniques in ECG signals, in: 2022 IEEE conference on telecommunications, Optics and Computer Science (TOCS), IEEE, Dalian, China, 2022: pp. 237–240. https://doi.org/10.1109/TOCS56154.2022.10015982.

[22] A.A. Ismael, M. Baykara, Digital image denoising techniques based on multi-resolution wavelet domain with spatial filters: A review, Trait. Signal 38 (2021) 639-651. https://doi.org/10.18280/ts.380311.

[23] A. Halidou, Y. Mohamadou, A.A.A. Ari, E.J.G. Zacko, Review of wavelet denoising algorithms, Multimed Tools Appl. (2023). https://doi.org/10.1007/s11042-023-15127-0.

[24] T. Guo, T. Zhang, E. Lim, M. Lopez-Benitez, F. Ma, L. Yu, A review of wavelet analysis and its applications: challenges and opportunities, IEEE Access 10 (2022) 58869-58903. https://doi.org/10.1109/ACCESS.2022.3179517.

[25] N. Prashar, M. Sood, S. Jain, Design and implementation of a robust noise removal system in ECG signals using dual-tree complex wavelet transform, Biomed. Signal Process. 63 (2021) 102212. https://doi.org/10.1016/j.bspc.2020.102212.

[26] G. Baldazzi, E. Sulas, M. Urru, R. Tumbarello, L. Raffo, D. Pani, Wavelet denoising as a post-processing enhancement method for non-invasive foetal electrocardiography, Comput. Meth. Prog. Bio. 195 (2020) 105558. https://doi.org/10.1016/j.cmpb.2020.105558.

[27] A. Kumar, H. Tomar, V.K. Mehla, R. Komaragiri, M. Kumar, M. Kumar, Stationary wavelet transform based ECG signal denoising method, ISA T. 114 (2021) 251–262. https://doi.org/10.1016/j.isatra.2020.12.029.

[28] T. Mourad, ECG denoising based on 1-D double-density complex DWT and SBWT, in: The stationary bionic wavelet transform and its applications for ECG and speech processing, Springer International Publishing, Cham, 2022: pp. 31–50. https://doi.org/10.1007/978-3-030-93405-7_2.

[29] S. Banerjee, G.K. Singh, A new moving horizon estimation based real-time motion artifact removal from wavelet subbands of ECG signal using particle filter, J. Signal Process. Syst. (2023). https://doi.org/10.1007/s11265-023-01887-3.

[30] B. Chen, J. Cui, Q. Xu, T. Shu, H. Liu, Coupling denoising algorithm based on discrete wavelet transform and modified median filter for medical image, J. Cent. South Univ. 26 (2019) 120–131. https://doi.org/10.1007/s11771-019-3987-9.

[31] A.K. Dwivedi, H. Ranjan, A. Menon, P. Periasamy, et al., Noise reduction in ECG signal using combined ensemble empirical mode decomposition method with stationary wavelet transform, Circ. Syst. Signal Process. 40 (2021) 827–844. https://doi.org/10.1007/s00034-020-01498-4.

[32] M. Sraitih, Y. Jabrane, A denoising performance comparison based on ECG signal decomposition and local means filtering, Biomed. Signal Process. 69 (2021) 102903. https://doi.org/10.1016/j.bspc.2021.102903.

[33] Y. Li, Z. Su, K. Chen, W. Zhang, M. Du, Application of an EMG interference filtering method to dynamic ECGs based on an adaptive wavelet-wiener filter and adaptive moving average filter, Biomed. Signal Process. 72 (2022) 103344. https://doi.org/10.1016/j.bspc.2021.103344.

[34] X. Hu, Q. Yu, H. Yu, An ECG denoising method combining variational modal decomposition and wavelet soft threshold, Concurr. Comp-Pract. E. (2022) e7048. https://doi.org/10.1002/cpe.7048.

[35] H. Serhal, N. Abdallah, J.-M. Marion, P. Chauvet, M. Oueidat, A. Humeau-Heurtier, Overview on prediction, detection, and classification of atrial fibrillation using wavelets and AI on ECG, Comput. Bio. Med. 142 (2022) 105168. https://doi.org/10.1016/j.compbiomed.2021.105168.

[36] Y. Gao, Y. Li, Y. Zhu, C. Wu, D. Gu, Power quality disturbance classification under noisy conditions using adaptive wavelet threshold and DBN-ELM hybrid model, Electr. Pow. Syst. Res. 204 (2022) 107682. https://doi.org/10.1016/j.epsr.2021.107682.

[37] L. Gao, Y. Gan, J. Shi, A novel intelligent denoising method of ecg sig-

nals based on wavelet adaptive threshold and mathematical morphology, Appl. Intell. 52 (2022) 10270–10284. https://doi.org/10.1007/s10489-022-03182-3.

[38] V.A. Ardeti, V.R. Kolluru, G.T. Varghese, R.K. Patjoshi, An overview on state-of-the-art electrocardiogram signal processing methods: Traditional to AI-based approaches, Expert Syst. Appl. 217 (2023) 119561. https://doi.org/10.1016/j.eswa.2023.119561.

[39] M. Malik, T. Dua, Snigdha, Biomedical signal processing: ECG signal analysis using machine learning in MATLAB, in: S. Yadav, K.P. Chaudhary, A. Gahlot, Y. Arya, A. Dahiya, N. Garg (Eds.), Recent advances in metrology, Springer Nature Singapore, Singapore, 2023: pp. 121–127. https://doi.org/10.1007/978-981-19-2468-2_14.

[40] S. Phadikar, N. Sinha, R. Ghosh, Automatic eyeblink artifact removal from EEG signal using wavelet transform with heuristically optimized threshold, IEEE J. Biomed. Health Inform. 25 (2021) 475-484. https://doi.org/10.1109/JBHI.2020.2995235.

[41] F. Zaki, Y. Wang, H. Su, X. Yuan, X. Liu, Noise adaptive wavelet thresholding for speckle noise removal in optical coherence tomography, Biomed. Opt. Express. 8 (2017) 2720. https://doi.org/10.1364/BOE.8.002720.

[42] M. Ghorat, G.B. Gharehpetian, H. Latifi, M.A. Hejazi, A New Partial Discharge Signal Denoising Algorithm Based on Adaptive Dual-Tree Complex Wavelet Transform, IEEE Trans. Instrum. Meas. 67 (2018) 2262–2272. https://doi.org/10.1109/TIM.2018.2816438.

[43] F.M. Bayer, A.J. Kozakevicius, R.J. Cintra, An iterative wavelet threshold for signal denoising, Signal Process. 162 (2019) 10–20. https://doi.org/10.1016/j.sigpro.2019.04.005.

[44] P. Madan, V. Singh, D.P. Singh, M. Diwakar, A. Kishor, A. Kishor, Denoising of ECG signals using weighted stationary wavelet total variation, Biomed. Signal Process. 73 (2022) 103478. https://doi.org/10.1016/j.bspc.2021.103478.

[45] S. Chatterjee, R.S. Thakur, R.N. Yadav, L. Gupta, Sparsity-based modified wavelet de-noising autoencoder for ECG signals, Signal Process. 198 (2022) 108605. https://doi.org/10.1016/j.sigpro.2022.108605.

[46] C. Chen, M. Shu, S. Zhou, Z. Liu, R. Liu, Wavelet-domain group-sparse denoising method for ECG signals, Biomed. Signal. Process. 83 (2023) 104702. https://doi.org/10.1016/j.bspc.2023.104702.

[47] R. Fu, J. Zhang, R. Wang, T. Xu, "Improved Wavelet Thresholding Function and Adaptive Thresholding for Noise Reduction," 2023 11th International Conference on Intelligent Computing and Wireless Optical Communications (ICWOC), Chongqing, China, 2023: pp. 25-30. https://doi.org/10.1109/ICWOC57905.2023.10200530.

[48] S.A. Malik, S.A. Parah, H. Aljuaid, B.A. Malik, An ierative filtering based ECG denoising using lifting wavelet transform technique, Electronics 12 (2023) 387. https://doi.org/10.3390/electronics12020387

[49] S. Poornachandra, Wavelet-based denoising using subband dependent threshold for ECG signals, Digit. Signal Process. 18 (2008) 49–55. https://doi.org/10.1016/j.dsp.2007.09.006.

[50] G.B. Moody, R.G. Mark, The impact of the MIT-BIH arrhythmia database, IEEE Eng. Med. Biol. Mag. 20 (2001) 45-50. https://doi.org/10.1109/51.932724.

[51] M. Wu, Y. Chen, P. Zhu, W. Chen, NLM parameter optimization for φ-OTDR signal, J. Lightwave Technol. 40 (2022) 6045-6051. https://doi.org/10.1109/JLT.2022.3186830.

[52] Y. Chen, P. Zhu, Y. Yin, M. Wu, K. Yu, L. Feng, W. Chen, Objective assessment of IPM denoising quality of φ-OTDR signal, Measurement 214 (2023) 112775. https://doi.org/10.1016/j.measurement.2023.112775.

[53] A. Martini, A. Rivola, M. Troncossi, Autocorrelation analysis of vibro-acoustic signals measured in a test field for water leak detection, Appl. Sci. 8 (2018) 2450. https://doi.org/10.3390/app8122450.

[54] R.-P. Nikula, K. Karioja, M. Pylvänäinen, K. Leiviskä, Automation of low-speed bearing fault diagnosis based on autocorrelation of time domain features, Mech. Syst. Signal Pr. 138 (2020) 106572. https://doi.org/10.1016/j.ymssp.2019.106572.

[55] S.S. Roy, S. Dey, S. Chatterjee, Autocorrelation aided random forest classifier-based bearing fault detection framework, IEEE Sens. J. 20 (2020) 10792-10800. https://doi.org/10.1109/JSEN.2020.2995109.

[56] Y. Xu, D. Zhen, J.X. Gu, K. Rabeyee, F. Chu, F. Gu, A.D. Ball, Autocorrelated Envelopes for early fault detection of rolling bearings, Mech. Syst. Signal Pr. 146 (2021) 106990. https://doi.org/10.1016/j.ymssp.2020.106990.

[57] A.R. Abbasi, M.R. Mahmoudi, M.M. Arefi, Transformer winding faults detection based on time series analysis, IEEE Trans. Instrum. Meas. 70 (2021) 1-10. https://doi.org/10.1109/TIM.2021.3076835.

[58] H. Wu, C. Shang, K. Zhu, C. Lu, Vibration detection in distributed acoustic sensor with threshold-based technique: A statistical view and analysis, J. Lightwave Technol. 39 (2021) 4082-4093. https://doi.org/10.1109/JLT.2020.3036450.

[59] F.M. Nolle, F.K. Badura, J.M. Catlett, R.W. Bowser, M.H. Sketch, CREI-GARD, a new concept in computerized arrhythmia monitoring systems. Computers in Cardiology 13 (1986) 515-518.

[60] R. Bousseljot, D. Kreiseler, A. Schnabel, Nutzung der EKG-signaldatenbank CARDIODAT der PTB über das internet, Biomed. Tech. (1995) 317-318. https://doi.org/10.1515/bmte.1995.40.s1.317.

[61] G.B. Moody, W.E. Muldrow, R.G. Mark, A noise stress test for arrhythmia detectors, Computers in Cardiology 11 (1984) 381-384.